



Cite this: *J. Mater. Chem. B*, 2021, 9, 7117

## Manganese oxide nanomaterials boost cancer immunotherapy

Binbin Ding,<sup>†a</sup> Jun Yue,<sup>ib†b</sup> Pan Zheng,<sup>ac</sup> Ping'an Ma<sup>ib\*ad</sup> and Jun Lin<sup>ib\*ad</sup>

Immunotherapy, a strategy that leverages the host immune function to fight against cancer, plays an increasingly important role in clinical tumor therapy. In spite of the great success achieved in not only clinical treatment but also basic research, cancer immunotherapy still faces many huge challenges. Manganese oxide nanomaterials (MONs), as ideal tumor microenvironment (TME)-responsive biomaterials, are able to dramatically elicit anti-tumor immune responses in multiple ways, indicating great prospects for immunotherapy. In this review, on the basis of different mechanisms to boost immunotherapy, major highlighted topics are presented, covering adjusting an immunosuppressive TME by generating O<sub>2</sub> (like O<sub>2</sub>-sensitized photodynamic therapy (PDT), programmed cell death ligand-1 (PD-L1) expression downregulation, reprogramming tumor-associated macrophages (TAMs), and restraining tumor angiogenesis and lactic acid exhaustion), inducing immunogenic cell death (ICD), photothermal therapy (PTT) induction, activating the stimulator of interferon gene (STING) pathway and immunoadjuvants for nanovaccines. We hope that this review will provide holistic understanding about MONs and their application in cancer immunotherapy, and thus pave the way to the translation from bench to bedside in the future.

Received 5th May 2021,  
Accepted 25th June 2021

DOI: 10.1039/d1tb01001h

rs.li/materials-b

<sup>a</sup> State Key Laboratory of Rare Earth Resource Utilization, Changchun Institute of Applied Chemistry, Chinese Academy of Sciences, Changchun, 130022, China.

E-mail: mapa675@ciac.ac.cn, jlin@ciac.ac.cn

<sup>b</sup> School of Biomedical Engineering, Sun Yat-sen University, Guangzhou, 510006, China

<sup>c</sup> Institute of Frontier and Interdisciplinarity Science and Institute of Molecular Sciences and Engineering, Shandong University, Qingdao, 266237, China

<sup>d</sup> University of Science and Technology of China, Hefei, 230026, China

<sup>†</sup> Binbin Ding and Jun Yue contributed equally to this work.

### 1. Introduction

Different from traditional surgery, chemotherapy and radiotherapy, immunotherapy, a strategy that leverages the host immune function to fight against cancer, plays an increasingly important role in clinical tumor therapy and is considered as one of the most promising treatments for curing cancer thanks to its abscopal effects that inhibit and eradicate



Binbin Ding

Binbin Ding was born in Anhui, China, in 1991. He received his BS degree (2015) in Pharmaceutical Engineering from Hefei University of Technology, and his PhD degree (2020) in Inorganic Chemistry under the guidance of Prof. Jun Lin at Changchun Institute of Applied Chemistry, Chinese Academy of Sciences. After graduation, he became Assistant Professor in Prof. Jun Lin's group. His current research focuses on the synthesis and bioapplication of nanoadducts.



Jun Yue

Jun Yue was born in He'nan, China, in 1983. He received his BS degree in Polymer Materials and Engineering from Zhengzhou University (2007) and PhD degree in Polymer Chemistry and Physics from Changchun Institute of Applied Chemistry (2013). From December 2012 to February 2018, he experienced postdoctoral work in Prof. A. Herrmann's group at the University of Groningen and Prof. Teri Odom's group at Northwestern University, respectively.

From March 2018, he was appointed as an associate professor in Biomedical Engineering at Sun Yat-sen University and presently his research interest is focused on the nanofabrication of novel biomaterials for cancer treatment and bioimaging.

metastatic tumors.<sup>1–5</sup> Currently, various strategies for immunotherapy are being developed, such as adoptive cell therapy, immune checkpoint blockade (ICB) therapy, cancer vaccine therapy and so on.<sup>6–10</sup> However, in spite of the great success achieved to date in not only clinical treatment but also basic research, cancer immunotherapy still faces many huge challenges, like low response rates, severe treatment-associated adverse effects, acquired immunological tolerance and so forth.<sup>11</sup> Furthermore, the complicated cancer-immunity cycle process and the immunosuppressive tumor microenvironment can further hinder the course of immunotherapy.<sup>12</sup> Encouragingly, the development of materials science and nanotechnology offers new opportunities and prospects for cancer immunotherapy.<sup>13–17</sup> To date, multifarious nanomaterials have been fabricated to boost anti-tumor immunotherapy through various mechanisms, which include three major strategies: nanomaterial-mediated combination therapy, adjustment of the immunosuppressive tumor microenvironment and construction of nanovaccines.<sup>18–22</sup>

In the past two decades, increasing attention has been paid to manganese oxide nanomaterials (MONs) and their derivatives

in biomedical applications, including bioimaging, biosensing, drug delivery and tumor therapy due to their excellent biosecurity and unique physical/chemical properties.<sup>23–27</sup> MONs are able to catalyze H<sup>+</sup>/hydrogen peroxide (H<sub>2</sub>O<sub>2</sub>) to oxygen (O<sub>2</sub>) and Mn<sup>2+</sup>, and oxidize glutathione (GSH) into oxidized glutathione (GSSH).<sup>28–30</sup> As is well known, the tumor microenvironment (TME) characteristically displays hypoxia, mild acidity, and GSH/H<sub>2</sub>O<sub>2</sub> overproduction.<sup>31,32</sup> Therefore, MONs as ideal TME-responsive biomaterials were designed to enhance the therapeutic efficiency by adjusting the immunosuppressive tumor microenvironment. For example, by overcoming tumor hypoxia, MONs can dramatically promote the tumor ablation in photodynamic therapy (PDT),<sup>33</sup> sonodynamic therapy (SDT),<sup>34</sup> and radiotherapy (RT).<sup>35</sup> In addition, it has been proved that MONs can be used directly for photothermal therapy (PTT),<sup>36</sup> ferroptosis,<sup>37</sup> chemodynamic therapy (CDT),<sup>38</sup> immunotherapy,<sup>39</sup> *etc.* Overall, manganese oxide-based nanomaterials hold great promise and have made huge progress in biomedical applications, particularly in tumor therapy. Some recent reviews by different groups including ours have outlined the progress in synthesis, properties, imaging, biodetection and therapeutic applications of MONs.<sup>40–43</sup> However, a comprehensive and specialized review on MONs for cancer immunotherapy has not been reported yet.

Inspired by the significant headway and great prospects of MONs in immunotherapy, herein, this review aims to provide a comprehensive overview of MONs and their derivatives for cancer immunotherapy. On the basis of different mechanisms to boost immunotherapy, major highlighted topics are presented, covering adjusting an immunosuppressive TME by generating O<sub>2</sub> (like O<sub>2</sub>-sensitized PDT, programmed cell death ligand-1 (PD-L1) expression downregulation, reprogramming tumor-associated macrophages (TAMs), and restraining tumor angiogenesis and lactic acid exhaustion), inducing immunogenic cell death (ICD), PTT induction, activating the stimulator of interferon gene (STING) pathway and immunoadjuvants for nanovaccines



**Pan Zheng**

*Pan Zheng was born in Anhui, China, in 1991. She received her BS degree (2015) in pharmaceutical engineering from Hefei University of Technology, and her PhD degree (2021) in Polymer Chemistry and Physics under the guidance of Prof. Gao Li at Changchun Institute of Applied Chemistry, Chinese Academy of Sciences. Her current research focuses on the design and preparation of activatable nanomaterials for cancer treatment.*



**Ping'an Ma**

*Ping'an Ma was born in Jilin, China, in 1982. He received his BS degree in Biology in 2005 at Northeast Normal University, and his PhD degree in Biochemistry in 2010 at Northeast Normal University. After graduation, he became Assistant Professor in Prof. Jun Lin's group and was promoted to Professor in 2020. His research focuses on the synthesis and application of multifunctional inorganic nanoparticles for bioapplication, particularly the design and mechanism of platinum-based anticancer drugs.*



**Jun Lin**

*Jun Lin was born in Changchun, China, in 1966. He received BS and MS degrees in Jilin University, and a PhD degree in Changchun Institute of Applied Chemistry (1995). His postdoctoral studies were performed at the City University of Hong Kong (1996), Institute of New Materials (Germany, 1997), Virginia Commonwealth University (USA, 1998), and the University of New Orleans (USA, 1999). He has been working as a Professor at CIAC since 2000. His research interests include bulk- and nanostructured luminescent materials and multifunctional composite materials, together with their applications in display, lighting, and biomedical fields.*



**Scheme 1** Schematic illustration of boosting cancer immunotherapy *via* manganese oxide nanomaterials by various mechanisms. Remarks: glutathione (GSH), oxidized glutathione (GSSH), photothermal therapy (PTT), photodynamic therapy (PDT), hypoxia inducible factor-1 $\alpha$  (HIF-1 $\alpha$ ), tumor-associated macrophages (TAM), programmed cell death ligand-1 (PD-L1), immunogenic cell death (ICD), chemodynamic therapy (CDT), and stimulator of interferon genes (STING).

**Table 1** Comparisons of different mechanisms of MONs for cancer immunotherapy

| Category                                  | Mechanisms                               | Materials   | Main functions  | Cells      | Ref. |
|---|--|---|---|------------|------|
| Adjusting TME by producing O <sub>2</sub> | O <sub>2</sub> -Sensitized PDT           | Au@MnO <sub>2</sub>   | Improving PDT efficiency to promote PDT-activated immune responses  | 4T1        | 44   |
|   | PD-L1 expression downregulation          | BSA-MnO <sub>2</sub> -IPI549  | Reducing HIF-1 $\alpha$ expression, which can selectively upregulate PD-L1                                | 4T1        | 45   |
|   | Reprogramming TAMs                       | PEG-modified Ce6/DOX-loaded hollow MnO <sub>2</sub>                             | Improving PDT efficiency and inducing TAM polarization from M2 to M1                                      | 4T1        | 46   |
|   | Restraining tumor angiogenesis           | MnO <sub>2</sub> @PLGA-sorafenib  | Inducing TAM polarization from M2 to M1 and promoting sorafenib-induced decrease in tumor vascularization | Murine HCC | 47   |
|   | Lactic acid exhaustion                   | mRBC-coated lactate oxidase/glycolysis inhibitor-loaded hollow MnO <sub>2</sub> | Promoting lactate oxidase-mediated oxidation reaction of lactic acid                                      | B16F10     | 48   |
| ICD induction                             | CDT and ferroptosis-induced ICD          | MnO <sub>x</sub>  | Mn <sup>2+</sup> -mediated CDT <i>via</i> Fenton-like reactions and GSH-depleting ferroptosis             | 4T1        | 49   |
|   | ICD under nutrient-deprived conditions   | MnO <sub>2</sub>  | Might elicit the autophagy machinery that in turn contributes to induction of ICD                         | 4T1        | 50   |
| PTT activation                            | PTT induces ICD                          | MnO <sub>2</sub> -based nanogels  | As a photothermal agent to achieve PTT-triggered antigens release   | 4T1        | 39   |
| Activating STING pathway                  | Mn <sup>2+</sup> Activates STING pathway | CM-coated MnO <sub>2</sub>  | Increase the pH value of TME, alleviate tumor hypoxia and activate STING pathway                          | B16F10     | 51   |
| Immunoadjuvant                            | Adjuvant effect                          | MnO <sub>x</sub>  | As an immunoadjuvant for antigen delivery   | 4T1        | 49   |

Remarks: tumor microenvironment (TME), photodynamic therapy (PDT), immunogenic cell death (ICD), photothermal therapy (PTT), stimulator of interferon genes (STING), tumor associated macrophages (TAMs), bovine serum albumin (BSA), polyethylene glycol (PEG), lipid-poly(lactic-co-glycolic) acid (PLGA), red blood cell membrane (mRBC), hypoxia inducible factor-1 $\alpha$  (HIF-1 $\alpha$ ), cancer cell membrane (CM).

(Scheme 1 and Table 1). Finally, the current challenges and future directions of MONs for immunotherapy are further discussed. We believe that this review will bring more inspirations to not only cancer immunotherapy but also the further application and conversion of manganese oxide-related nanoplatfoms.

## 2. Adjusting immunosuppressive TME by generating O<sub>2</sub>

The outcome of immunotherapy is greatly limited to immunosuppressive TME. For instance, hypoxia, a characteristic feature of solid tumors, can bring about a series of adverse consequences

on antitumor immune response, including upregulations of PD-L1 and tumor invasion-related signaling molecules like vascular endothelial growth factor (VEGF), which are mainly involved in angiogenesis and metastasis.<sup>45,52</sup> Therefore, it is very necessary and important to modify immunosuppressive conditions and reshape the tumor immune microenvironment. As an excellent endogenous O<sub>2</sub> donor by reacting with H<sub>2</sub>O<sub>2</sub>/H<sup>+</sup>, manganese oxide-based nano-systems show superior ability for adjusting immunosuppressive TME by overcoming tumor hypoxia.

## 2.1 O<sub>2</sub>-Sensitized PDT

Classical PDT, a noninvasive therapy modality based on the photochemical reactions of photosensitizers (PSs) to generate cytotoxic intracellular reactive oxygen species (ROS), is an effective cancer therapeutic strategy.<sup>53,54</sup> In particular, it has been demonstrated that PDT could not only kill cancer cells directly, but also elicit antitumor immune responses *via* release of tumor-associated antigens (TAAs), also called ICD.<sup>55–58</sup> However, tumor hypoxia greatly limits the efficiency of O<sub>2</sub>-dependent PDT.<sup>59</sup> MONs can tremendously enhance PDT efficiency by reacting with H<sub>2</sub>O<sub>2</sub>/H<sup>+</sup> to produce O<sub>2</sub>, and thus promote antitumor immunity.

A representative example was presented by the Cai group, in which they prepared core-shell gold nanocage@manganese dioxide (AuNC@MnO<sub>2</sub>, AM) nanoparticles as tumor microenvironment-responsive O<sub>2</sub> producers and near-infrared (NIR)-triggered ROS generators for O<sub>2</sub>-sensitized immunogenic PDT (Fig. 1a and b).<sup>44</sup> As shown in Fig. 1c, compared with other groups, enhanced ROS contents were observed in the AM + laser group, indicating that O<sub>2</sub>

produced by MnO<sub>2</sub> can promote PDT. Next, the markers of ICD as a cornerstone of therapy-induced antitumor immunity were further tested and the results reveal that the AM + laser group can induce the most conspicuous calreticulin (CRT) exposure and adenosine triphosphate (ATP)/high mobility group protein B1 (HMGB1) release (Fig. 1d–f). The elevated immune response was examined by dendritic cells (DCs) maturity and interleukin 12 (IL-12) secretion using co-cultivation of mouse bone marrow-derived dendritic cells (BMDCs) and 4T1 cells (Fig. 1g and h). Next, *in vivo* study confirmed that AM under 808 nm laser irradiation not only ablated the primary tumor directly but also inhibited tumor metastasis and recurrence. In addition, the authors also found that AM can relieve tumor hypoxia by *in situ* oxygenation to remodel the immunosuppressive TME by decreasing regulatory T cell (Treg) expression. Similarly, other groups also reported that enhanced antitumor immunity can be achieved by O<sub>2</sub>-sensitized PDT.<sup>60–66</sup>

## 2.2 PD-L1 expression downregulation

Hypoxia-inducible factor-1 $\alpha$  (HIF-1 $\alpha$ ) selectively up-regulates PD-L1 by binding to the hypoxia response elements (HRE) in the PD-L1 proximal promoter, which dampens the antitumor immune response.<sup>67,68</sup> Hence, MONs as an O<sub>2</sub> supplier can reduce PD-L1 expression by overcoming tumor hypoxia to boost immunotherapy. Based on this, Yu and co-workers prepared a multifunctional nanoregulator incorporating MnO<sub>2</sub> particles and small molecular IPI549 (BMI) to reshape the tumor immune microenvironment (TIME) as displayed in Fig. 2.<sup>45</sup> Here, IPI549, as a small molecular gamma isoform of phosphoinositide 3-kinase

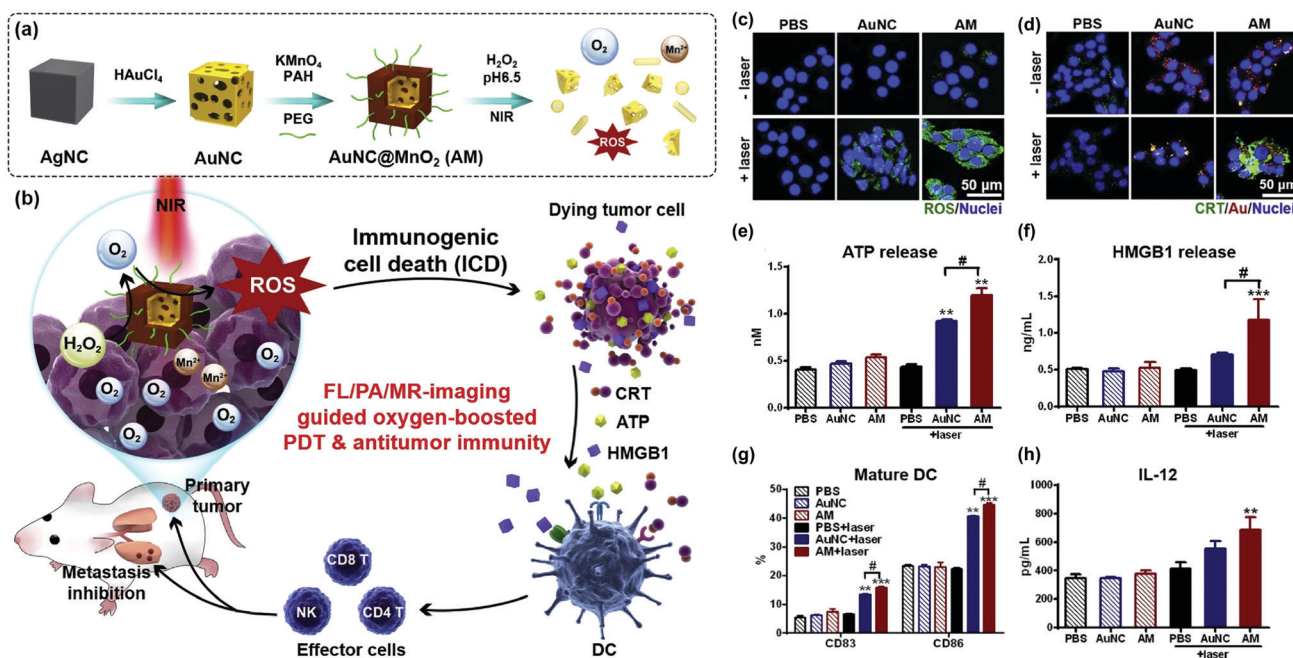


Fig. 1 (a) Preparation procedure of core-shell gold nanocage@manganese dioxide (AuNC@MnO<sub>2</sub>, AM) and its applications in acid/H<sub>2</sub>O<sub>2</sub>-responsive oxygen-boosted PDT. (b) The therapeutic mechanism of AM for multimodal imaging-guided oxygen-boosted PDT. (c) ROS detection in 4T1 cells after treatment with AM and 808 nm laser irradiation (0.8 W cm<sup>-2</sup>, 3 min) by confocal microscopy. (d) Immunofluorescence microscopy of CRT expression on 4T1 cell surface after treatment with AM and laser irradiation. (e) Released ATP in the supernatant. (f) Released HMGB1 in the supernatant. (g) The expression of CD83 and CD86 of mature DC stimulated by ICD signal molecules. (h) Production of IL-12 in the culture supernatant. The asterisks indicate that differences between PBS and other treatments are statistically significant. \*\**p* < 0.01, \*\*\**p* < 0.001. Reproduced with permission.<sup>44</sup> Copyright 2018, Elsevier.

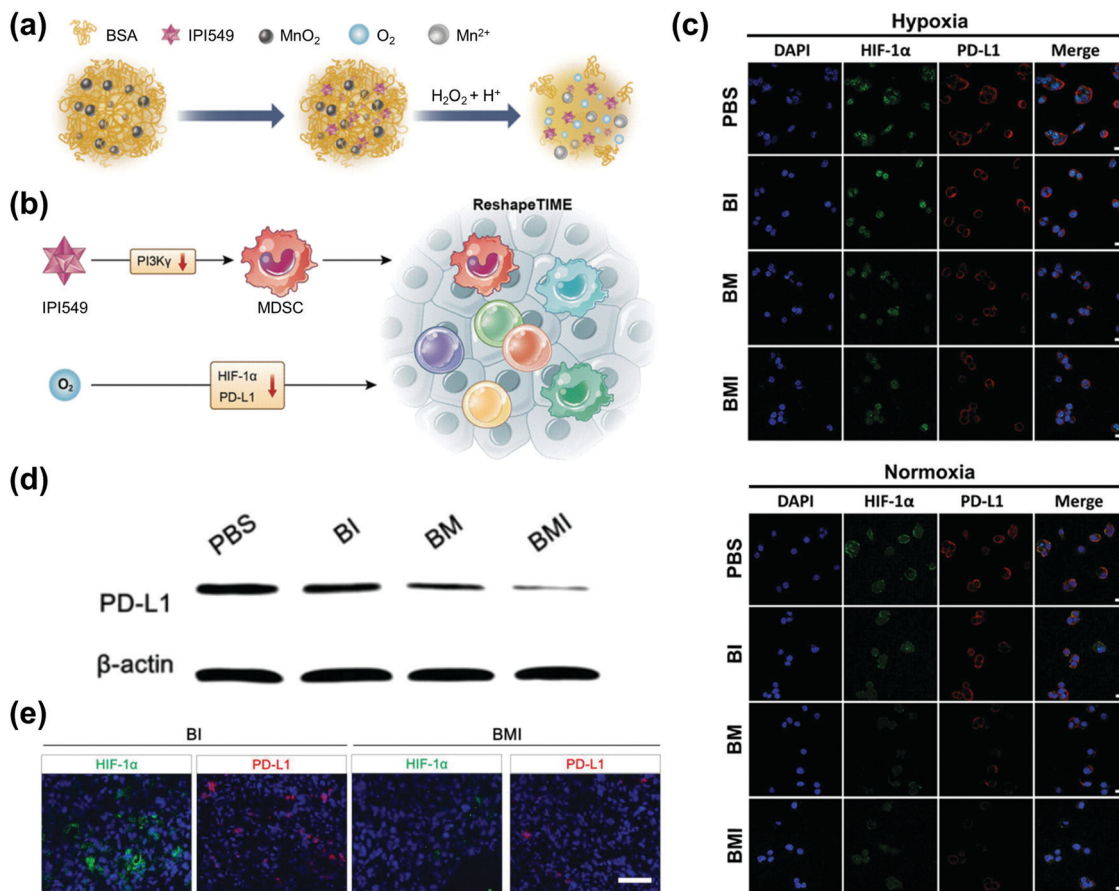


Fig. 2 (a) A scheme showing the pH/H<sub>2</sub>O<sub>2</sub> responsiveness of bovine serum albumin (BSA)-MnO<sub>2</sub>-IPI549 (BMI). (b) Schematic illustration of reshaping the tumor immune microenvironment (TIME) by a pluripotent nanoregulator. (c) Immunofluorescence analysis of HIF-1 $\alpha$  and PD-L1 expressions of 4T1 cells after incubation for 24 h with different formulations (200  $\mu$ g mL<sup>-1</sup>) under hypoxia and normoxia conditions, respectively. (d) Western blot analysis of PD-L1 protein in 4T1 tumors collected from mice on the 18 d during treatment. (e) Immunofluorescence assays displaying HIF-1 $\alpha$  sections from mice after drug withdrawal. Reproduced with permission.<sup>45</sup> Copyright 2019, Wiley-VCH.

(PI3K $\gamma$ ) inhibitor, can switch macrophages from the immunosuppressive M2-like phenotype to the pro-inflammatory M1-like state. Due to the synergistic effect of hypoxia alleviation *via* oxygen-generating reduction of MnO<sub>2</sub> and PI3K $\gamma$  inhibition, the nanoplatform achieved concurrent downregulation of PD-L1 expression and polarization of tumor associated macrophages (TAMs), suggesting effective tumor immunotherapy. Fig. 2c–e show that MnO<sub>2</sub>-embedded nanoregulators resulted in a significant down-regulation of HIF-1 $\alpha$  and PD-L1 expressions *via* immunofluorescence staining and western blotting assay.

The residual HIF-1 $\alpha$  will further dimerize with HIF-1 $\beta$  to form HIF-1 and activate tumor invasion-related signaling molecules like VEGF and matrix metalloproteinase 9 (MMP-9). The Yuan group demonstrated that the expression of tumor invasion-related signaling molecules (VEGF and MMP-9) was obviously decreased under down-regulation of HIF-1 by the introduction of MnO<sub>2</sub> nanoparticles, which helps to reduce the risk of metastasis.<sup>52</sup>

### 2.3 Reprogramming TAMs

Normally, macrophages can be divided into two subtypes, the classically activated pro-inflammatory (M1) phenotype (attacking

invaders) and the alternatively activated anti-inflammatory (M2) phenotype (healing damages).<sup>69</sup> It has been revealed that M2 phenotype TAMs support tumor progression *via* secretion of pro-tumor cytokines such as IL-10, and thereby promote tissue repair and tumor recurrence including angiogenesis, matrix remodeling, and immunosuppression.<sup>70,71</sup> In contrast, M1 phenotype TAMs exhibit classic antitumor activity by producing multiple cytotoxic cytokines like tumor necrosis factor alpha (TNF- $\alpha$ ) and IL-6.<sup>72,73</sup> Another strategy of adjusting immunosuppressive TME by MONs and their derivatives is to reprogram TAMs *via* the transformation of the M2 to the M1 phenotype.<sup>69</sup> A typical example developed by the Liu group showed that polyethylene glycol (PEG)-modified chlorine e6 (Ce6)/doxorubicin (DOX)-loaded hollow manganese dioxide (H-MnO<sub>2</sub>-PEG/C&D) was prepared for combination therapy favoring antitumor immune responses (Fig. 3a and b).<sup>46</sup> Here, the tumor hypoxia was relieved by MnO<sub>2</sub>-mediated decomposition of endogenous H<sub>2</sub>O<sub>2</sub> inside tumors, which not only improved the efficacy of chemo-PDT, but also reversed the immunosuppressive TME to favor anti-tumor immunity post treatment. Under an oxygen atmosphere and 660 nm light irradiation, both free Ce6 and Ce6-loaded MnO<sub>2</sub> nanoparticles exhibited high cytotoxicity.

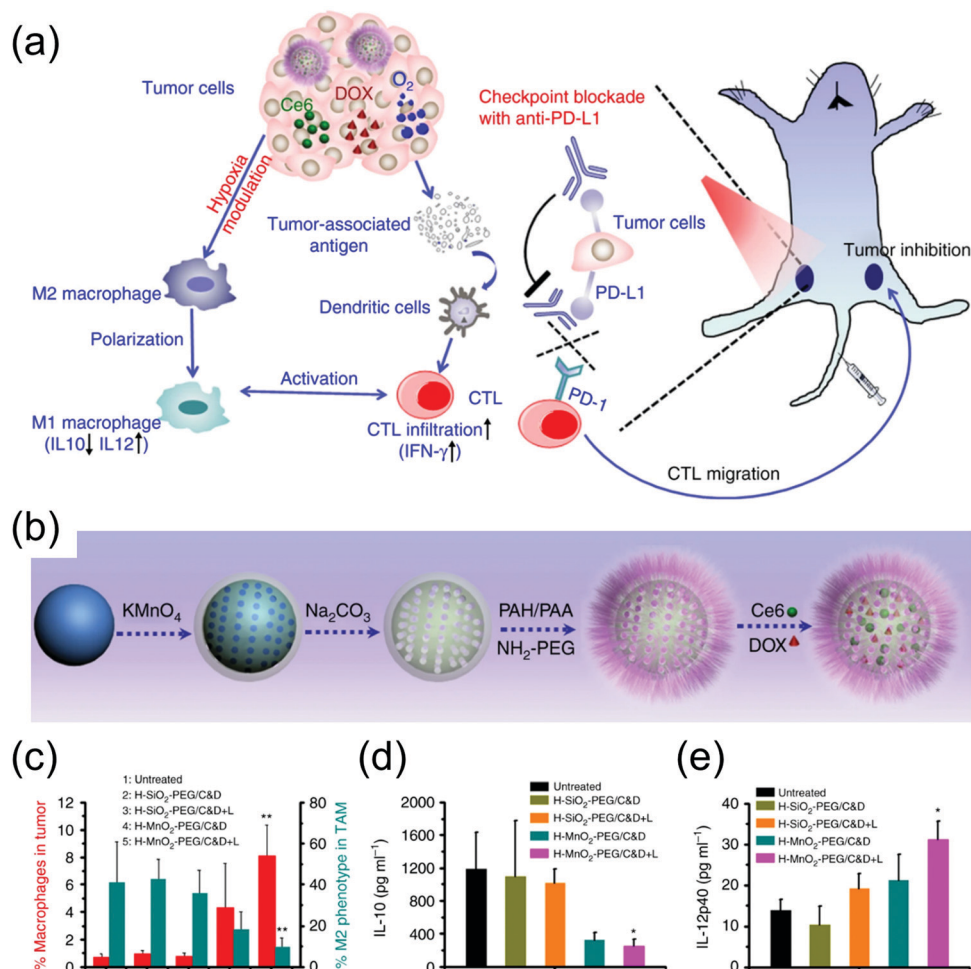


**Fig. 3** (a) The proposed mechanism of anti-tumor immune responses induced by polyethylene glycol (PEG)-modified chlorine e6 (Ce6)/doxorubicin (DOX)-loaded hollow manganese dioxide (H-MnO<sub>2</sub>-PEG/C&D) in combination with anti-PD-L1 therapy. (b) A scheme indicating the step-by-step synthesis of H-MnO<sub>2</sub>-PEG nanoparticles and the subsequent dual-drug loading. (c) Macrophage infiltration and polarization within tumors post various treatments. CD11b<sup>+</sup>CD206<sup>+</sup> cells were defined as M2 phenotype macrophages (six mice per group). The total number of macrophages infiltrated in tumors markedly increased after the combined chemo-PDT, which also resulted in polarization of M2 phenotype TAM towards M1 TAM. The levels of IL-10 (d) and IL-12p40 (e) in the supernatant of tumors post various treatments. Reproduced with permission.<sup>46</sup> Copyright 2017, Springer Nature.

However, the phototoxicity of free Ce6 was found to be significantly lower, while the cell killing efficiency of Ce6-loaded MnO<sub>2</sub> nanoparticles remained at high levels under hypoxic conditions. What's more, as displayed in Fig. 3c, compared with the untreated group, tumors in mice with i.v. injection of H-MnO<sub>2</sub>-PEG/C&D plus light irradiation showed markedly elevated macrophage infiltration within tumors from 0.8% to 8%, together with reduced population of M2 phenotype TAMs from 40% to 9.5% among all the TAMs. Furthermore, in the H-MnO<sub>2</sub>-PEG/C&D-injected mice under light exposure, the secretion of IL-10 in the supernatant of tumor lysates also decreased by 3.77 times (Fig. 3d); however, the content of IL-12 in tumors presented a significant increase (Fig. 3e), both suggesting remarkable M2 to M1 polarization within tumors.

#### 2.4 Restraining tumor angiogenesis

The formation of blood vessels that supply nutrients and oxygen is very important for solid tumor growth and progression.

Therefore, based on the vital function of abnormal vessels in the TME, anti-angiogenic therapy has become a widely studied therapeutic strategy.<sup>74–76</sup> Sorafenib, as an anti-angiogenic agent, has been approved by the US Food and Drug Administration (FDA). However, hypoxia can result in severe resistance to sorafenib.<sup>77</sup> To overcome this challenge, Chang *et al.* prepared NanoMnSor, which is composed of a MnO<sub>2</sub> core and a lipid-poly(lactic-co-glycolic) acid (PLGA) shell loaded with sorafenib (Fig. 4).<sup>47</sup> The authors confirmed that this nanomaterial is not only able to promote macrophage polarization toward the immunostimulatory M1 phenotype, but also leads to sorafenib-induced decrease in tumor vascularization by generating abundant O<sub>2</sub>. Additionally, the NanoMnSor treatment can reverse hypoxia-induced cell invasion and epithelial-to-mesenchymal transition (EMT), and thus significantly inhibit tumor metastasis. In brief, this study demonstrates the potential of oxygen-generating NanoMnSor, efficiently boosting anti-angiogenic therapy and immune responses. A similar result was also reported by He *et al.* and

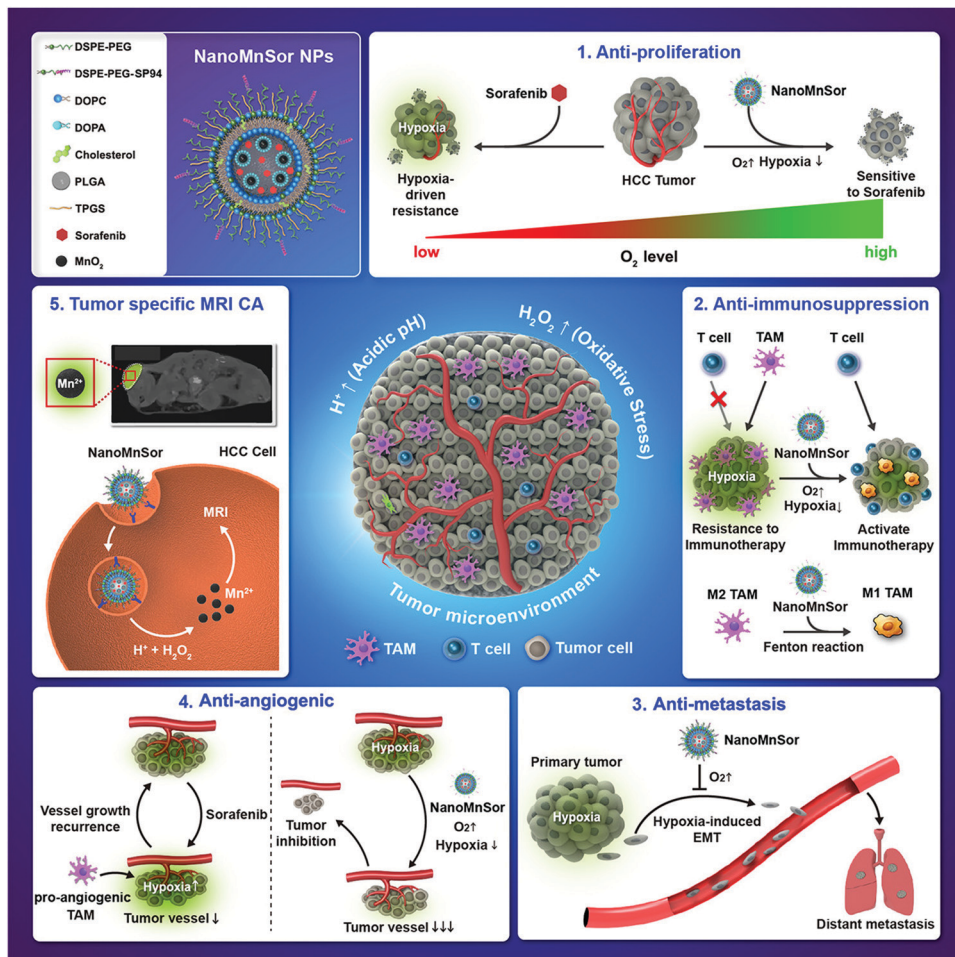


Fig. 4 Schematic representation of the mechanism by which NanoMnSor can serve as a theranostic anticancer agent. Oxygen generated from NanoMnSor, which is composed of a  $\text{MnO}_2$  core and a lipid-poly(lactic-co-glycolic acid) (PLGA) shell loaded with sorafenib, alleviates tumor hypoxia and modulates the TME. (1) NanoMnSor treatment overcomes hypoxia-driven resistance to sorafenib and reduces cancer cell proliferation in hepatocellular carcinoma (HCC). (2) NanoMnSor ameliorates the immunosuppressive TME by reducing the hypoxia-induced tumor infiltration of TAMs. (3) NanoMnSor suppresses metastasis in HCC by attenuating hypoxia-induced epithelial-to-mesenchymal transition (EMT). (4) NanoMnSor treatment enhances antiangiogenic effect of sorafenib *via* hypoxia alleviation. (5) NanoMnSor potentially serves as a magnetic resonance imaging (MRI) contrast agent (CA). Reproduced with permission.<sup>47</sup> Copyright 2020, American Chemical Society.

bovine serum albumin (BSA)-modified sorafenib/Ce6-co-loaded  $\text{MnO}_2$  nanocomposites were obtained to relieve immunosuppression during long-term anti-angiogenesis therapy.<sup>62</sup>

### 2.5 Lactic acid exhaustion

Lactic acid, the most ubiquitous component of TME, is ceaselessly produced by the aerobic glycolysis of tumor cells for energy production. It has been confirmed that the mass of lactic acid is adverse to antitumor immunotherapy.<sup>78–80</sup> To this end, the Zhang group proposed an innovative intra/extracellular lactic acid exhaustion strategy for synergistic antitumor metabolic therapy and ICB therapy.<sup>48</sup> Firstly, red blood cell membrane (mRBC)-encapsulated 3-(3-pyridinyl)-1-(4-pyridinyl)-2-propen-1-one (3PO, glycolysis inhibitor)/lactate oxidase (LOX)-co-loaded hollow  $\text{MnO}_2$  ( $\text{HMnO}_2$ ) nanoparticles (denoted as PMLR) were synthesized as presented in Fig. 5a. In this work, LOX was introduced to catalyze the oxidation reaction of lactic acid with  $\text{O}_2$ , and the byproduct

could be further catalyzed by  $\text{HMnO}_2$  to generate  $\text{O}_2$  for lactic acid oxidation (Fig. 5b–d). At the same time, the intracellular nanosystem can further release the glycolysis inhibitor to interdict the source of lactic acid and ATP supply for antitumor metabolic therapy. The data showed that the PMLR nanosystem could ceaselessly remove lactic acid, and then bring about an immunocompetent TME and notably enhance the efficiency of anti-PD-L1 therapy.

## 3. ICD induction

The dying tumor cells after drug treatment can generate damage-associated molecular patterns (DAMPs), including CRT, heat shock proteins (HSP70 and HSP90), HMGB1, and ATP, which can further stimulate the engulfment of dying tumor cells by immature DCs, resulting in DC maturation.<sup>81–84</sup> This functionally peculiar type of cell death is termed “ICD”.<sup>85,86</sup> As mentioned

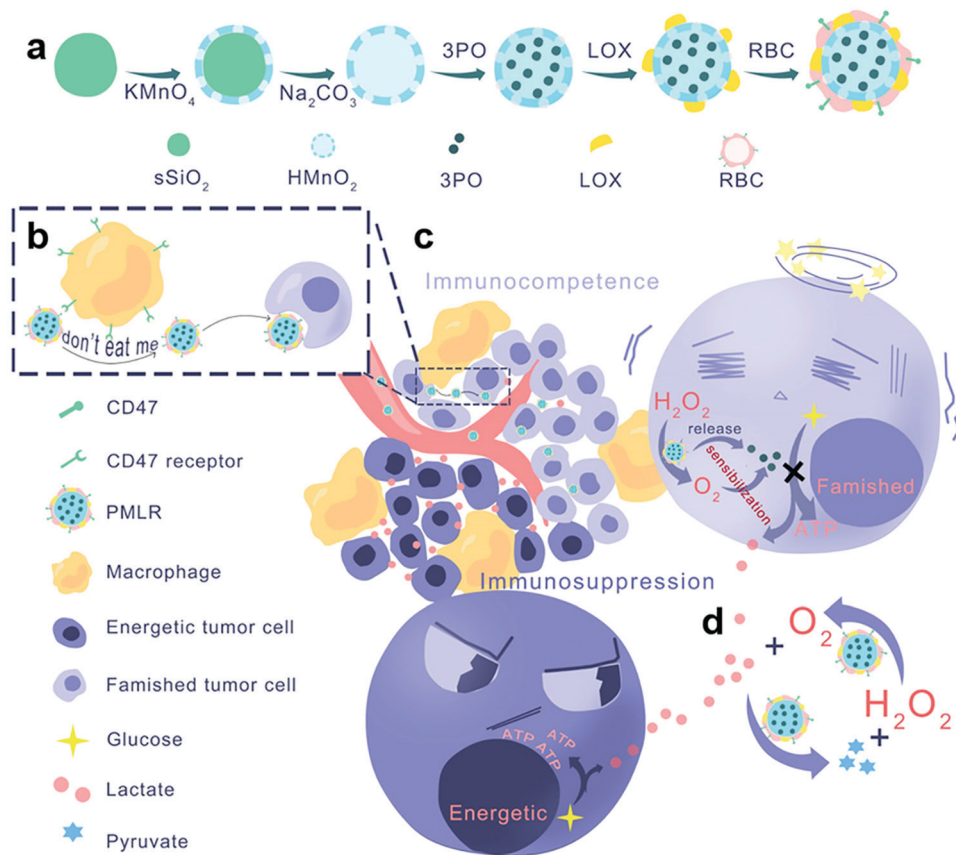


Fig. 5 Schematic illustration of the intra/extracellular lactic acid exhaustion process of the PMLR nanosystem. (a) Preparation steps of the PMLR nanosystem. (b) The mRBC-camouflaged nanosystem can avoid the phagocytosis of macrophages through the CD47-mediated “don’t eat me” signal. (c) PMLR nanosystem releases 3PO to inhibit the glycolysis of tumor cells and catalyzes the decomposition of endogenous  $\text{H}_2\text{O}_2$  to sensitize the 3PO. This process cuts off the source of ATP and lactic acid. (d) Cascade catalysis process of the PMLR nanosystem. The PMLR nanosystem catalyzes the oxidation process of extracellular lactic acid to generate pyruvate and  $\text{H}_2\text{O}_2$ , the latter of which can be further converted into  $\text{O}_2$  to accelerate the lactic acid oxidation process. Reproduced with permission.<sup>48</sup> Copyright 2019, Wiley-VCH.

above, manganese oxide-based nanoplatfoms play a subsidiary role in assisting PDT-induced ICD by creating a favorable micro-environment. However, the intrinsic immunogenicity and ICD induction of MONs are still unclear. Until recently, as far as we know, our group first demonstrated that MONs can intrinsically induce ICD *via* CDT and ferroptosis inductions due to highly efficient  $\cdot\text{OH}$  generation and GSH depletion capabilities.<sup>49</sup> After that, the Yu group also found that  $\text{MnO}_2$  nanoflowers (MNFs) can efficiently induce ICD in cancer cells under nutrient-deprived conditions (Fig. 6a and b).<sup>50</sup> The two studies help to break the stereotype of the subsidiary role of MONs in cancer immunotherapy. As exhibited in Fig. 6c and d, compared with the groups treated with full media, amino-acid-deprived ( $\text{AA}^-$ ) media and MNFs + full media, MNFs +  $\text{AA}^-$  media-incubated 4T1 cells showed significantly increased exposure level of ecto-CRT and ATP/HMGB1 release acting as “eat me” signals and “find me” signals, respectively. Next, the underlying mechanism of the MNF-mediated ICD under nutrient-deprived conditions was further studied and the authors explained that MNFs in nutrient deficiency might elicit the autophagy machinery that in turn contributes to the induction of ICD. Based on these findings, 5,6-dimethylxanthenone-4-acetic acid (DMXAA), a drug that

specifically targets endothelial cells and damages the tumor vasculature system (blood vessels) to cut off nutrient supply, was chosen for synergistic cancer starvation-immunotherapy in combination with MNFs.

## 4. PTT activation

It has been proved that PTT facilitates the *in situ* release of tumor-derived protein antigens (TDPAs) and other immune stimulating substances by eliciting the immunogenic death of autologous tumor cells, which can trigger a robust immune response.<sup>87–90</sup>  $\text{MnO}_2$  nanomaterials with intense absorption in the near infrared region possess photothermal conversion capability and can be used for PTT.<sup>36,91</sup> Hence, MONs are capable of activating antitumor immunity by releasing autologous antigens *via* PTT induction. A recent example reported by Fan *et al.* reveals this process well.<sup>39</sup> As shown in Fig. 7a, thermosensitive poly(*N*-isopropylacrylamide-co-dopamine methacrylamide) (PND) nanogels were synthesized firstly and then  $\text{MnO}_2$  nanoparticles ( $\text{MnO}_2$  NPs) were formed in the network of the PND nanogels ( $\text{MnO}_2$ @PND) *via* an *in situ* mineralization process.



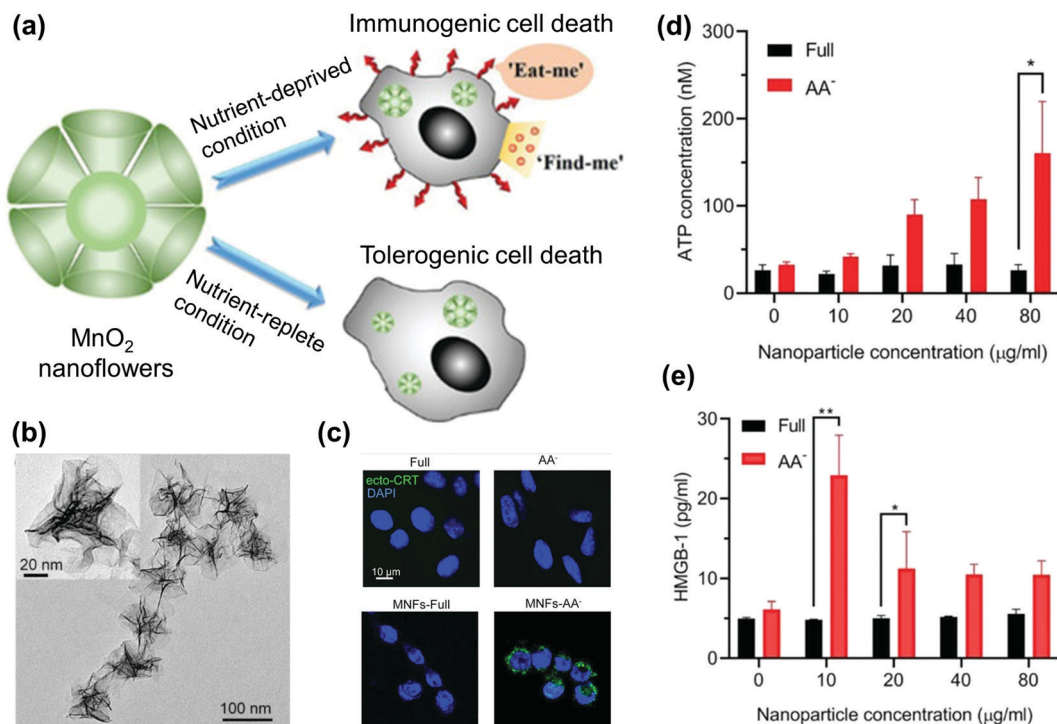


**Fig. 6** (a) Schematic illustration of MnO<sub>2</sub> nanoflowers (MNFs) for nutrient-dependent immunogenic cell death (ICD). (b) Transmission electron microscopy (TEM) image of MnO<sub>2</sub> nanoflowers. (c) Confocal laser scanning microscopy (CLSM) image of the surface exposure of ecto-CRT on 4T1 cells. 4T1 cells were cultured in full media, amino-acid-deprived (AA<sup>-</sup>) media, MNFs + full media, and MNFs + AA<sup>-</sup> media, respectively. (d and e) Secretion of ATP and HMGB-1 in the cell culture media. Reproduced with permission.<sup>50</sup> Copyright 2020, Wiley-VCH.

The photothermal effect of MnO<sub>2</sub> NPs induced ICD to release mass autologous TDPAs under near-infrared irradiation. At the same time, an injectable hydrogel like an “antigen reservoir” can capture the antigens generated by PTT due to the existence of catechol groups, and thus achieve lasting anti-tumor immune response (Fig. 7b). Under continuous 808 nm laser irradiation (1.0 W cm<sup>-2</sup>) for 10 min, the temperature changes ( $\Delta T$ ) of PBS and PND dispersions were smaller than 8 °C, while the  $\Delta T$  of the MnO<sub>2</sub>@PND dispersion (100 mg mL<sup>-1</sup>) achieved was up to 34 °C, suggesting that the photothermal effects were originated from MnO<sub>2</sub> NPs. The photothermal conversion efficiency ( $\eta$ ) of MnO<sub>2</sub>@PND was determined to be 33.2%. Furthermore, under 808 nm laser irradiation, MnO<sub>2</sub>@PND-treated cells showed the highest level of CRT exposure and the highest release of HMGB1. *In vivo* study demonstrated that the obtained MnO<sub>2</sub>@PND nanogels eliminated the primary tumors completely and effectively suppressed distal/rechallenged tumors, showing great potential in PTT-induced immunotherapy.

## 5. Activating the STING pathway

The cyclic GMP-AMP synthase (cGAS)/STING pathway, as an endogenous mechanism in an innate immune system, can activate antitumor immune responses through the spontaneous secretion of type I interferon (IFN-I) and pro-inflammatory cytokines.<sup>92,93</sup> Recently, increasing attention has been paid to STING-mediated stimulation of the innate immune system because it is very

important for spontaneous induction of antitumor T-cell immunity.<sup>94,95</sup> Meanwhile, it should be noted that Mn<sup>2+</sup> ions in the cytoplasm as an alarmin and an activator in innate immune system, have potential to activate intracellular STING pathway.<sup>96,97</sup> Inspired by this, Hou *et al.* constructed doxorubicin (DOX)-loaded and phospholipid (PL)-coated amorphous porous manganese phosphate (APMP) nanoparticles (PL/APMP-DOX NPs).<sup>98</sup> After systemic administration, this nanomaterials release DOX for inducing DNA damage and Mn<sup>2+</sup> to augment cGAS/STING activity, and thus promote DC maturation, cytotoxic T lymphocyte (CTL) induction, natural killer cell (NK) recruitment, and type I IFN/TNF- $\alpha$  expressions, indicating that this innate immunity nanoactivator has the potential to amplify antitumor immunotherapeutic efficacy. Using a similar principle, Sun and co-workers developed a straight and versatile strategy for *in situ* STING-activating vaccination (ISSAV) by converting a primary tumor towards a therapeutic STING vaccine.<sup>51</sup> For this purpose, they prepared cancer cell membrane (CM)-encapsulated MnO<sub>2</sub> NPs and immobilized photothermal agent (DiR) (CMM-DiR). As presented in Fig. 8a–d, on the one hand, CMM-DiR induced the exposure of numerous TAAs by hyperthermia, thus transforming the primary tumors into TAAs. On the other hand, CMM-DiR realized burst release of Mn<sup>2+</sup> to activate the STING pathway and build a therapeutic STING vaccine in conjunction with TAAs. Accordingly, the primary tumor possessed the dual functions as adequate antigens and STING agonist depots. Additionally, the degradation of MnO<sub>2</sub> also generated numerous O<sub>2</sub> and increased the pH value of TME, which was more conducive to

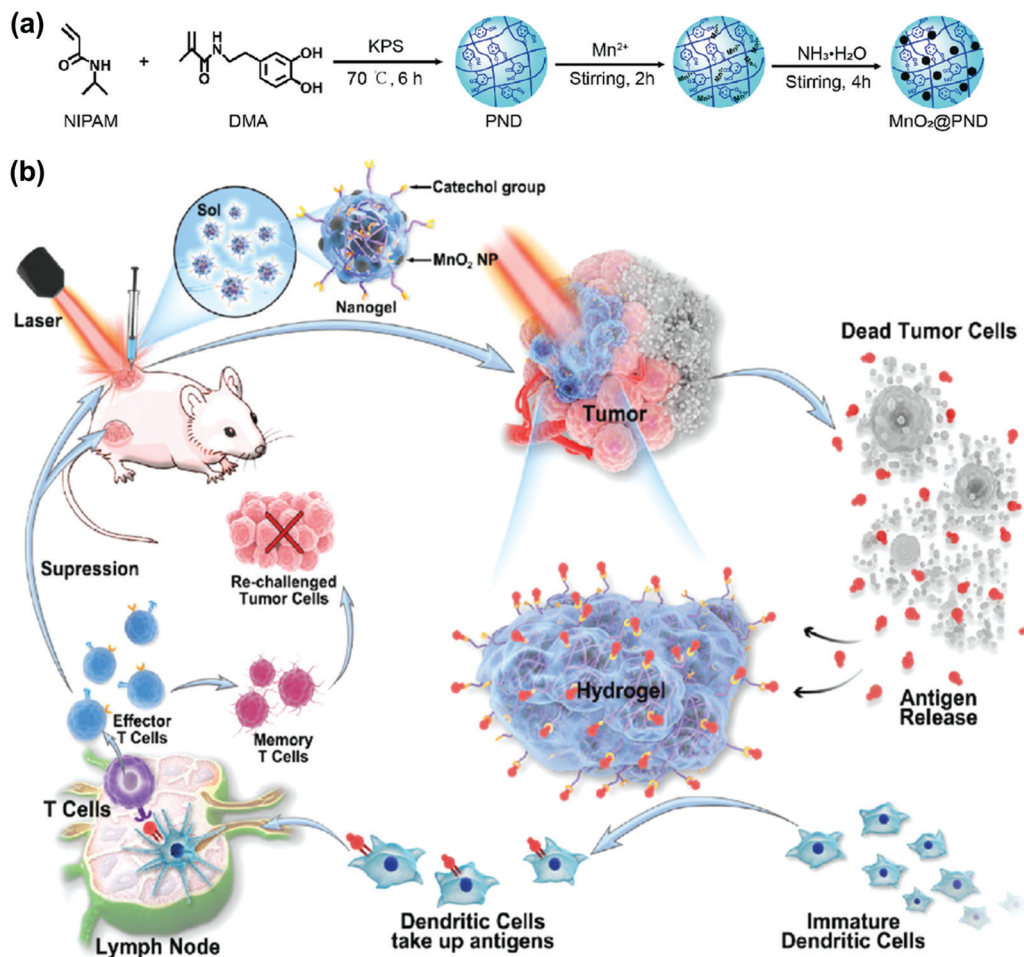


Fig. 7 (a) Schematic showing the preparation of the poly(*N*-isopropylacrylamide-co-dopamine methacrylamide) (PND) and MnO<sub>2</sub>@PND nanogels. (b) Schematic illustration of the mechanism of "antigen reservoir" formation and the anti-tumor immune response to inhibit the growth of primary tumor, distal tumor, and rechallenged tumor. Reproduced with permission.<sup>39</sup> Copyright 2021, Wiley-VCH.

the infiltration of the T lymphocyte. In short, the ISSAV proposed by this paper brings inspiration for cancer vaccinations and personalized immunotherapy.

## 6. Immunoadjuvant

Immunoadjuvant refers to a substance which is injected into the body prior to the antigen or after mixing with antigen, which can non-specifically change or enhance the body's specific immune response to the antigen, and thus plays an adjuvant role.<sup>99–101</sup> Alum adjuvant, as the most widely used immunoadjuvant, has been applied in dozens of vaccine products.<sup>102,103</sup> However, the long-term retention effect and possible toxicity of aluminum adjuvants limit their future applications. Finding appropriate and safe immunoadjuvants has always been a major challenge. Inspired by biodegradable properties and the biosafety of MONs, our group first reported that MnO<sub>x</sub> nanospikes (NSs) can serve as immunoadjuvants for cancer nanovaccine-based immunotherapy (Fig. 9a–d).<sup>49</sup> Compared with traditional immunoadjuvants, using MnO<sub>x</sub> as

an immunoadjuvant has the following merits: (a) MnO<sub>x</sub> is biodegradable, avoiding *in vivo* long-term retention; (b) manganese is one of the essential elements in the human body and MnO<sub>x</sub> possesses good biosecurity; (c) MnO<sub>x</sub> can modulate immunosuppressive TME by the production of O<sub>2</sub> and the consumption of H<sup>+</sup>; (d) MnO<sub>x</sub> NSs with large mesopores structures show high antigen loading capacities; (e) MnO<sub>x</sub> can intrinsically induce ICD *via* CDT and ferroptosis induction, triggering dying tumor cells to generate DAMPs; (f) MnO<sub>x</sub> NSs display TME-responsive magnetic resonance (MR)/photoacoustic (PA) dual-mode imaging capacities. Moreover, MnO<sub>x</sub> NSs prepared by a fast aqueous phase synthesis method at room temperature avoids complicated nanomaterial modulation, which is beneficial for future applications. Next, *in vivo* tests further testified that the corporate administration of adjuvants and antigens showed the best DC maturity, T-cell activation, cytokine secretion and tumor growth inhibition in comparison with adjuvants and antigens alone, indicating that MnO<sub>x</sub> can act as an immunoadjuvant to enhance *in vivo* specific immune responses. Very recently, Chen's group also reported a new nanovaccine comprising the Receptor-Binding Domain (RBD) of the spike protein and the manganese

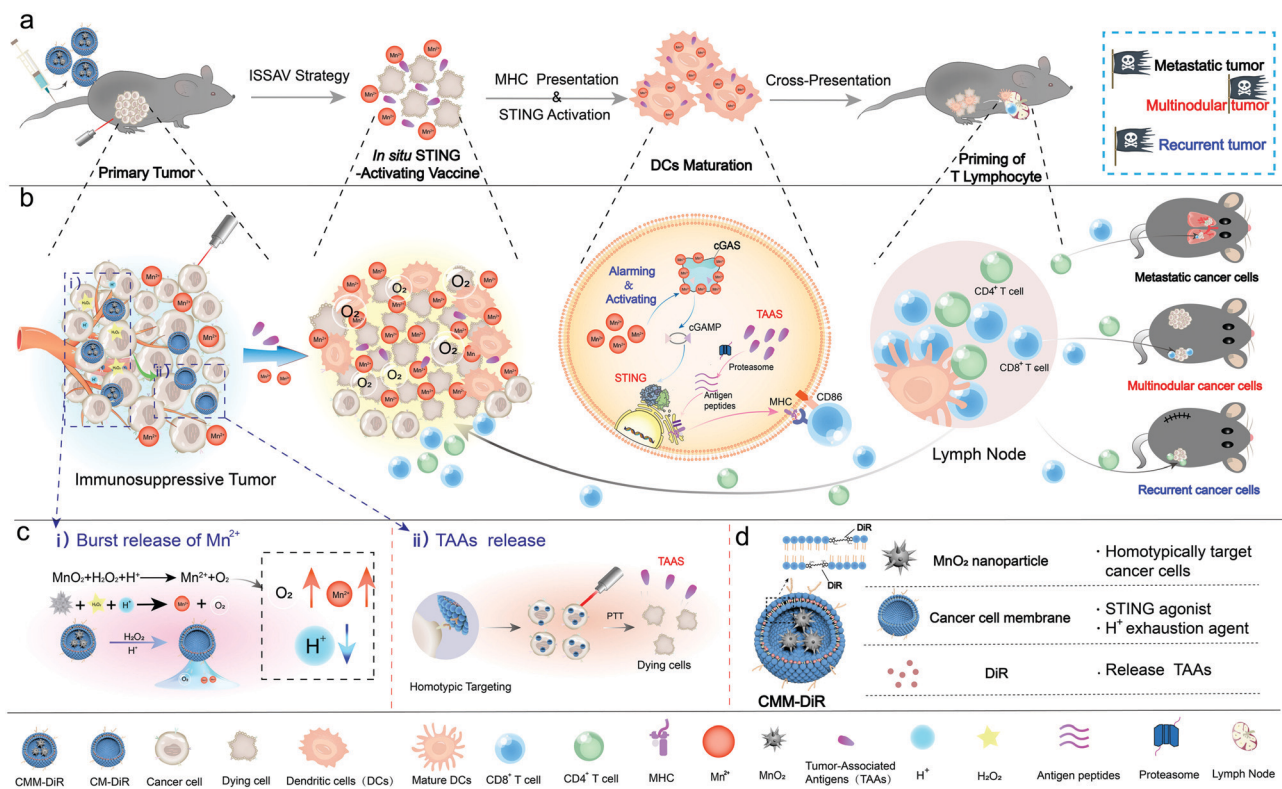


**Fig. 8** Schematic of the *in situ* STING-activating vaccination (ISSAV) strategy achieved using a biomimetic nanoplatform (CMM-DiR). (a) A schematic illustration of how the biomimetic nanoplatform converts immunosuppressive tumors towards the *in situ* STING-activating vaccine and elicits immune response. (b and c) The details of how ISSAV strategy works. Following intravenous administration, CMM-DiR was accumulated in the tumor. Then, the nanoplatform could be degraded quickly into  $Mn^{2+}$  and CM-DiR in TME, along with the production of  $O_2$  and the consumption of  $H^+$ . The remaining nanoplatform (CM-DiR) is taken up by the tumor cells through the homotypic adhesion property. Next, under laser irradiation, due to hyperthermia, tumor cells release a large number of TAAs, thus transforming the primary tumor into a STING-activating vaccine. This *in situ* STING vaccine can promote DC maturation through STING activation and MHC presentation. Finally, the mature DCs induce the priming of the T lymphocyte for combating incurable tumors (metastatic tumors, and multinodular and tumor recurrent tumors). (d) Composition of the nanoplatform (CMM-DiR) and the function of each component. Reproduced with permission.<sup>51</sup> Copyright 2021, Elsevier.

nanoadjuvant (MnARK) for inducing potent protective immunity against the novel coronavirus.<sup>104</sup> They found that even at a 5-fold lower antigen dose and with fewer injections, mice immunized with the MnARK vaccine displayed stronger neutralizing abilities against the infection of the pseudovirus ( $\sim 270$ -fold) and live coronavirus ( $> 8$ -fold) *in vitro* than that of Alum-adsorbed RBD vaccine (Alu-RBD). In brief, the above two works reveal that MONs as new-style immunoadjuvants are feasible and possess broad prospects in vaccines.

## 7. Conclusions and outlook

In this review, we have summarized the recent advances in MONs and their derivatives for cancer immunotherapy. According to the different mechanisms for boosting immunotherapy, major highlighted topics are introduced, such as the adjustment of an immunosuppressive TME by generating  $O_2$  (including  $O_2$ -sensitized PDT, PD-L1 expression downregulation, reprogramming tumor-associated macrophages, restraining tumor angiogenesis and lactic acid exhaustion), ICD induction,

PTT activation, activation of the STING pathway and immunoadjuvants for nanovaccines.

In short, MON-based nanoplatforms like an all-rounder are able to dramatically elicit anti-tumor immune responses in multiple ways, which have the most obvious advantages over other nanomaterials in cancer immunotherapy. Hence MONs can be designed to promote immune responses and therapeutic outcomes simultaneously through several mechanisms. For complex immune systems and TME, it is very important for obtaining an ideal treatment effect. Additionally, we should also pay more attention to the latest discoveries about MONs in immunotherapy, including activation of the STING pathway and serving as immunoadjuvants for nanovaccines. Do manganese adjuvants become the next generation of adjuvants like classical aluminium adjuvants? It may be an important one of the future research directions. Furthermore, some other challenges still persist and remain to be solved, like large-scale production, potential toxicity analysis, in-depth study of MON-related immune mechanisms and so on. It is very urgent and highly desired that multidisciplinary cooperation will promote a more rapid clinical translation of MONs. We hope

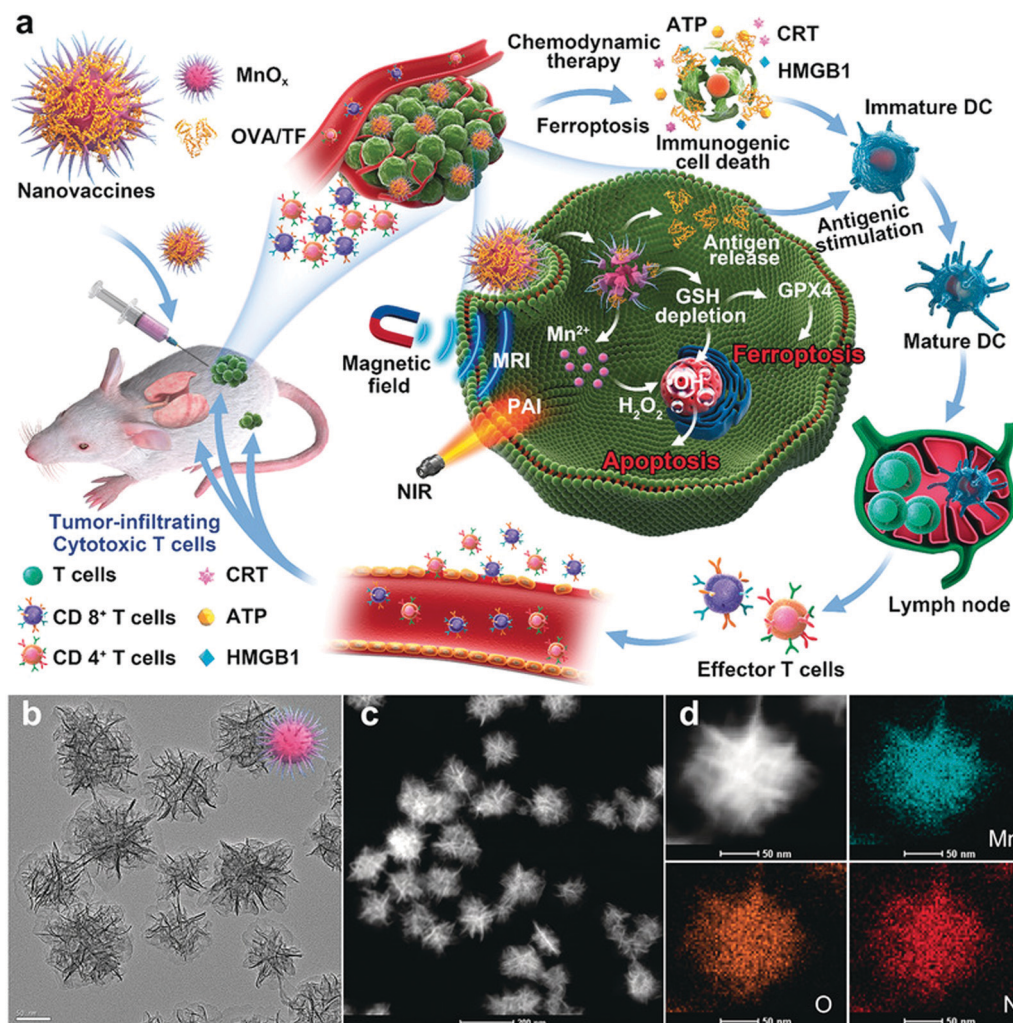


Fig. 9 (a) Illustration of  $\text{MnO}_x$ -OVA/tumor cell fragment (TF) nanovaccines for MR/PA dual-mode imaging-induced cancer immunotherapy. (b) TEM and (c) scanning TEM (STEM) images of  $\text{MnO}_x$  NSs. (d) Elemental mapping of  $\text{MnO}_x$ -OVA. Reproduced with permission.<sup>49</sup> Copyright 2020, Wiley-VCH.

that this review will provide a holistic understanding about MONs and their application in cancer immunotherapy, and thus pave the way to the bench to bedside translation in the future.

## Conflicts of interest

The authors declare no conflict of interest.

## Acknowledgements

This work is financially supported by the Science and Technology Cooperation Project between Chinese and Australian Governments (2017YFE0132300), the National Natural Science Foundation of China (Grant No. NSFC 51720105015, 51929201, 51922097, 51772124 and 51872282), the Key Research Program of Frontier Sciences, CAS (YZDY-SSW-JSC018), the Postdoctoral Innovative Talents Support Program (BX2021360) and the Youth Innovation Promotion Association of CAS (Grant No. 2017273).

## References

- 1 Y. Min, K. C. Roche, S. Tian, M. J. Eblan, K. P. McKinnon, J. M. Caster, S. Chai, L. E. Herring, L. Zhang, T. Zhang, J. M. DeSimone, J. E. Tepper, B. G. Vincent, J. S. Serody and A. Z. Wang, *Nat. Nanotechnol.*, 2017, **12**, 877–882.
- 2 M. Luo, H. Wang, Z. Wang, H. Cai, Z. Lu, Y. Li, M. Du, G. Huang, C. Wang, X. Chen, M. R. Porembka, J. Lea, A. E. Frankel, Y.-X. Fu, Z. J. Chen and J. Gao, *Nat. Nanotechnol.*, 2017, **12**, 648–654.
- 3 I. Mellman, G. Coukos and G. Dranoff, *Nature*, 2011, **480**, 480–489.
- 4 S. A. Rosenberg, J. C. Yang and N. P. Restifo, *Nat. Med.*, 2004, **10**, 909–915.
- 5 T. N. Schumacher and R. D. Schreiber, *Science*, 2015, **348**, 69–74.
- 6 Q. Chen, M. Chen and Z. Liu, *Chem. Soc. Rev.*, 2019, **48**, 5506–5526.
- 7 D. B. Keskin, A. J. Anandappa, J. Sun, I. Tirosh, N. D. Mathewson, S. Li, G. Oliveira, A. Giobbie-Hurder, K. Felt,

- E. Gjini, S. A. Shukla, Z. Hu, L. Li, P. M. Le, R. L. Allesoe, A. R. Richman, M. S. Kowalczyk, S. Abdelrahman, J. E. Geduldig, S. Charbonneau, K. Pelton, J. B. Iorgulescu, L. Elagina, W. Zhang, O. Olive, C. McCluskey, L. R. Olsen, J. Stevens, W. J. Lane, A. M. Salazar, H. Daley, P. Y. Wen, E. A. Chiocca, M. Harden, N. J. Lennon, S. Gabriel, G. Getz, E. S. Lander, A. Regev, J. Ritz, D. Neuberg, S. J. Rodig, K. L. Ligon, M. L. Suva, K. W. Wucherpfennig, N. Hacohen, E. F. Fritsch, K. J. Livak, P. A. Ott, C. J. Wu and D. A. Reardon, *Nature*, 2019, **565**, 234–239.
- 8 U. Sahin, P. Oehm, E. Derhovanessian, R. A. Jabulowsky, M. Vormehr, M. Gold, D. Maurus, D. Schwarck-Kokarakis, A. N. Kuhn, T. Omokoko, L. M. Kranz, M. Diken, S. Kreiter, H. Haas, S. Attig, R. Rae, K. Cuk, A. Kemmer-Brueck, A. Breikreuz, C. Tolliver, J. Caspar, J. Quinkhardt, L. Hebich, M. Stein, A. Hohberger, I. Vogler, I. Liebig, S. Renken, J. Sikorski, M. Leierer, V. Mueller, H. Mitzel-Rink, M. Miederer, C. Huber, S. Grabbe, J. Utikal, A. Pinter, R. Kaufmann, J. C. Hassel, C. Loquai and O. Tuereci, *Nature*, 2020, **585**, 107–112.
- 9 X. Han, H. Li, D. Zhou, Z. Chen and Z. Gu, *Acc. Chem. Res.*, 2020, **53**, 2521–2533.
- 10 D. M. Pardoll, *Nat. Rev. Cancer*, 2012, **12**, 252–264.
- 11 C. Zhang and K. Pu, *Chem. Soc. Rev.*, 2020, **49**, 4234–4253.
- 12 S. Yan, Z. Luo, Z. Li, Y. Wang, J. Tao, C. Gong and X. Liu, *Angew. Chem., Int. Ed.*, 2020, **59**, 17332–17343.
- 13 Q. Sun, M. Barz, B. G. De Geest, M. Diken, W. E. Hennink, F. Kiessling, T. Lammers and Y. Shi, *Chem. Soc. Rev.*, 2019, **48**, 351–381.
- 14 W. Sang, Z. Zhang, Y. Dai and X. Chen, *Chem. Soc. Rev.*, 2019, **48**, 3771–3810.
- 15 W. Li, Z. Liu, F. Fontana, Y. Ding, D. Liu, J. T. Hirvonen and H. A. Santos, *Adv. Mater.*, 2018, **30**, 1703740.
- 16 H. Phuengkham, L. Ren, I. W. Shin and Y. T. Lim, *Adv. Mater.*, 2019, **31**, 1803322.
- 17 W. Song, S. N. Musetti and L. Huang, *Biomaterials*, 2017, **148**, 16–30.
- 18 Y. Shi and T. Lammers, *Acc. Chem. Res.*, 2019, **52**, 1543–1554.
- 19 M. E. Aikins, C. Xu and J. J. Moon, *Acc. Chem. Res.*, 2020, **53**, 2094–2105.
- 20 H. Cabral, H. Kinoh and K. Kataoka, *Acc. Chem. Res.*, 2020, **53**, 2765–2776.
- 21 A. S. Cheung and D. J. Mooney, *Nano Today*, 2015, **10**, 511–531.
- 22 R. H. Fang, A. V. Kroll and L. Zhang, *Small*, 2015, **11**, 5483–5496.
- 23 Z. Zhao, H. Fan, G. Zhou, H. Bai, H. Liang, R. Wang, X. Zhang and W. Tan, *J. Am. Chem. Soc.*, 2014, **136**, 11220–11223.
- 24 Y. Chen, D. Ye, M. Wu, H. Chen, L. Zhang, J. Shi and L. Wang, *Adv. Mater.*, 2014, **26**, 7019–7026.
- 25 J. Liu, L. Meng, Z. Fei, P. J. Dyson, X. Jing and X. Liu, *Biosens. Bioelectron.*, 2017, **90**, 69–74.
- 26 R. Deng, X. Xie, M. Vendrell, Y.-T. Chang and X. Liu, *J. Am. Chem. Soc.*, 2011, **133**, 20168–20171.
- 27 M. Song, T. Liu, C. Shi, X. Zhang and X. Chen, *ACS Nano*, 2016, **10**, 633–647.
- 28 W. Fan, W. Bu, B. Shen, Q. He, Z. Cui, Y. Liu, X. Zheng, K. Zhao and J. Shi, *Adv. Mater.*, 2015, **27**, 4155–4161.
- 29 H. Fan, G. Yan, Z. Zhao, X. Hu, W. Zhang, H. Liu, X. Fu, T. Fu, X.-B. Zhang and W. Tan, *Angew. Chem., Int. Ed.*, 2016, **55**, 5477–5482.
- 30 B. Ding, S. Shao, F. Jiang, P. Dang, C. Sun, S. Huang, P. A. Ma, D. Jin, A. A. A. Kheraif and J. Lin, *Chem. Mater.*, 2019, **31**, 2651–2660.
- 31 Z. Tang, H. Zhang, Y. Liu, D. Ni, H. Zhang, J. Zhang, Z. Yao, M. He, J. Shi and W. Bu, *Adv. Mater.*, 2017, **29**, 1701683.
- 32 S. Ruan, M. Yuan, L. Zhang, G. Hu, J. Chen, X. Cun, Q. Zhang, Y. Yang, Q. He and H. Gao, *Biomaterials*, 2015, **37**, 425–435.
- 33 W. Zhu, Z. Dong, T. Fu, J. Liu, Q. Chen, Y. Li, R. Zhu, L. Xu and Z. Liu, *Adv. Funct. Mater.*, 2016, **26**, 5490–5498.
- 34 Y. Zhang, Y. Xu, D. Sun, Z. Meng, W. Ying, W. Gao, R. Hou, Y. Zheng, X. Cai, B. Hu and X. Lin, *Chem. Eng. J.*, 2020, **390**, 124521.
- 35 X. Yi, L. Chen, X. Zhong, R. Gao, Y. Qian, F. Wu, G. Song, Z. Chai, Z. Liu and K. Yang, *Nano Res.*, 2016, **9**, 3267–3278.
- 36 L. Wang, S. Guan, Y. Weng, S.-M. Xu, H. Lu, X. Meng and S. Zhou, *ACS Appl. Mater. Interfaces*, 2019, **11**, 6267–6275.
- 37 S. Wang, F. Li, R. Qiao, X. Hu, H. Liao, L. Chen, J. Wu, H. Wu, M. Zhao, J. Liu, R. Chen, X. Ma, D. Kim, J. Sun, T. P. Davis, C. Chen, J. Tian, T. Hyeon and D. Ling, *ACS Nano*, 2018, **12**, 12380–12392.
- 38 L.-S. Lin, J. Song, L. Song, K. Ke, Y. Liu, Z. Zhou, Z. Shen, J. Li, Z. Yang, W. Tang, G. Niu, H.-H. Yang and X. Chen, *Angew. Chem., Int. Ed.*, 2018, **57**, 4902–4906.
- 39 M. Fan, L. Jia, M. Pang, X. Yang, Y. Yang, S. Kamel Elyzayati, Y. Liao, H. Wang, Y. Zhu and Q. Wang, *Adv. Funct. Mater.*, 2021, **31**, 2010587.
- 40 B. Ding, P. Zheng, P. A. Ma and J. Lin, *Adv. Mater.*, 2020, **32**, 1905823.
- 41 X. Qian, X. Han, L. Yu, T. Xu and Y. Chen, *Adv. Funct. Mater.*, 2020, **30**, 1907066.
- 42 D. Zhu, X.-H. Zhu, S.-Z. Ren, Y.-D. Lu and H.-L. Zhu, *J. Drug Target.*, 2020, DOI: 10.1080/1061186x.2020.1815209.
- 43 X. Liu, Y. Zhou, W. Xie, S. Liu, Q. Zhao and W. Huang, *Small Methods*, 2020, **4**, 2000566.
- 44 R. Liang, L. Liu, H. He, Z. Chen, Z. Han, Z. Luo, Z. Wu, M. Zheng, Y. Ma and L. Cai, *Biomaterials*, 2018, **177**, 149–160.
- 45 M. Yu, X. Duan, Y. Cai, F. Zhang, S. Jiang, S. Han, J. Shen and X. Shuai, *Adv. Sci.*, 2019, **6**, 1900037.
- 46 G. Yang, L. Xu, Y. Chao, J. Xu, X. Sun, Y. Wu, R. Peng and Z. Liu, *Nat. Commun.*, 2017, **8**, 902.
- 47 C.-C. Chang, D. Trinh Kieu, Y.-A. Lee, F.-N. Wang, Y.-C. Sung, P.-L. Yu, S.-C. Chiu, Y.-C. Shih, C.-Y. Wu, Y.-D. Huang, J. Wang, T.-T. Lu, D. Wan and Y. Chen, *ACS Appl. Mater. Interfaces*, 2020, **12**, 44407–44419.
- 48 F. Gao, Y. Tang, W.-L. Liu, M.-Z. Zou, C. Huang, C.-J. Liu and X.-Z. Zhang, *Adv. Mater.*, 2019, **31**, 1904639.
- 49 B. Ding, P. Zheng, F. Jiang, Y. Zhao, M. Wang, M. Chang, P. A. Ma and J. Lin, *Angew. Chem., Int. Ed.*, 2020, **59**, 16381–16384.

- 50 Y. Yang, Z. Gu, J. Tang, M. Zhang, Y. Yang, H. Song and C. Yu, *Adv. Sci.*, 2020, **8**, 2002667.
- 51 X. Yang, Y. Yang, J. Bian, J. Wei, Z. Wang, Z. Zhou, Z. Li and M. Sun, *Nano Today*, 2021, **38**, 101109.
- 52 L. Meng, Y. Cheng, X. Tong, S. Gan, Y. Ding, Y. Zhang, C. Wang, L. Xu, Y. Zhu, J. Wu, Y. Hu and A. Yuan, *ACS Nano*, 2018, **12**, 8308–8322.
- 53 C. He, X. Duan, N. Guo, C. Chan, C. Poon, R. R. Weichselbaum and W. Lin, *Nat. Commun.*, 2016, **7**, 12499.
- 54 D. Wang, T. Wang, J. Liu, H. Yu, S. Jiao, B. Feng, F. Zhou, Y. Fu, Q. Yin, P. Zhang, Z. Zhang, Z. Zhou and Y. Li, *Nano Lett.*, 2016, **16**, 5503–5513.
- 55 J. Xu, L. Xu, C. Wang, R. Yang, Q. Zhuang, X. Han, Z. Dong, W. Zhu, R. Peng and Z. Liu, *ACS Nano*, 2017, **11**, 4463–4474.
- 56 G. Lan, K. Ni, Z. Xu, S. S. Veroneau, Y. Song and W. Lin, *J. Am. Chem. Soc.*, 2018, **140**, 5670–5673.
- 57 K. Lu, C. He, N. Guo, C. Chan, K. Ni, R. R. Weichselbaum and W. Lin, *J. Am. Chem. Soc.*, 2016, **138**, 12502–12510.
- 58 A. P. Castano, P. Mroz and M. R. Hamblin, *Nat. Rev. Cancer*, 2006, **6**, 535–545.
- 59 H. Chen, J. Tian, W. He and Z. Guo, *J. Am. Chem. Soc.*, 2015, **137**, 1539–1547.
- 60 Y. Liu, Y. Pan, W. Cao, F. Xia, B. Liu, J. Niu, G. Alfranca, X. Sun, L. Ma, J. M. de la Fuente, J. Song, J. Ni and D. Cui, *Theranostics*, 2019, **9**, 6867–6884.
- 61 C.-H. Chung, K.-Y. Lu, W.-C. Lee, W.-J. Hsu, W.-F. Lee, J.-Z. Dai, P.-W. Shueng, C.-W. Lin and F.-L. Mi, *Biomaterials*, 2020, **257**, 120227.
- 62 Q. He, Z. Zhang, H. Liu, Z. Tuo, J. Zhou, Y. Hu, Y. Sun, C. Wan, Z. Xu, J. F. Lovell, D. Hu, K. Yang and H. Jin, *Nanoscale*, 2020, **12**, 14788–14800.
- 63 Y. Liu, J. Yang, B. Liu, W. Cao, J. Zhang, Y. Yang, L. Ma, J. M. de la Fuente, J. Song, J. Ni, C. Zhang and D. Cui, *Nano-Micro Lett.*, 2020, **12**, 127.
- 64 Z. Shen, J. Xia, Q. Ma, W. Zhu, Z. Gao, S. Han, Y. Liang, J. Cao and Y. Sun, *Theranostics*, 2020, **10**, 9132–9152.
- 65 C. Wang, Y. Xiao, W. Zhu, J. Chu, J. Xu, H. Zhao, F. Shen, R. Peng and Z. Liu, *Small*, 2020, **16**, 2000589.
- 66 L. Zhou, L. Chen, X. Hu, Y. Lu, W. Liu, Y. Sun, T. Yao, C. Dong and S. Shi, *Commun. Biol.*, 2020, **3**, 343.
- 67 I. B. Barsoum, C. A. Smallwood, D. R. Siemens and C. H. Graham, *Cancer Res.*, 2014, **74**, 665–674.
- 68 M. Z. Noman, G. Desantis, B. Janji, M. Hasmmim, S. Karray, P. Dessen, V. Bronte and S. Chouaib, *J. Exp. Med.*, 2014, **211**, 781–790.
- 69 X. Ai, M. Hu, Z. Wang, L. Lyu, W. Zhang, J. Li, H. Yang, J. Lin and B. Xing, *Bioconjugate Chem.*, 2018, **29**, 928–938.
- 70 S. Zanganeh, G. Hutter, R. Spitler, O. Lenkov, M. Mahmoudi, A. Shaw, J. S. Pajarinen, H. Nejadnik, S. Goodman, M. Moseley, L. M. Coussens and H. E. Daldrup-Link, *Nat. Nanotechnol.*, 2016, **11**, 986–994.
- 71 G.-T. Yu, L. Rao, H. Wu, L.-L. Yang, L.-L. Bu, W.-W. Deng, L. Wu, X. Nan, W.-F. Zhang, X.-Z. Zhao, W. Liu and Z.-J. Sun, *Adv. Funct. Mater.*, 2018, **28**, 1801389.
- 72 L. He, T. Nie, X. Xia, T. Liu, Y. Huang, X. Wang and T. Chen, *Adv. Funct. Mater.*, 2019, **29**, 1901240.
- 73 Y. Wang, Y.-X. Lin, S.-L. Qiao, H.-W. An, Y. Ma, Z.-Y. Qiao, R. P. Y. J. Rajapaksha and H. Wang, *Biomaterials*, 2017, **112**, 153–163.
- 74 G. Gu, Q. Hu, X. Feng, X. Gao, M. Jiang, T. Kang, D. Jiang, Q. Song, H. Chen and J. Chen, *Biomaterials*, 2014, **35**, 8215–8226.
- 75 Z. Wei, P. Liang, J. Xie, C. Song, C. Tang, Y. Wang, X. Yin, Y. Cai, W. Han and X. Dong, *Chem. Sci.*, 2019, **10**, 2778–2784.
- 76 P. Bhattarai, S. Hameed and Z. Dai, *Nanoscale*, 2018, **10**, 5393–5423.
- 77 Y.-j. Zhu, B. Zheng, H.-y. Wang and L. Chen, *Acta Pharmacol. Sin.*, 2017, **38**, 614–622.
- 78 J. X. Wang, S. Y. C. Choi, X. Niu, N. Kang, H. Xue, J. Killam and Y. Wang, *Int. J. Mole. Sci.*, 2020, **21**, 8363.
- 79 O. R. Colegio, C. Ngoc-Quynh, A. L. Szabo, T. Chu, A. M. Rhebergen, V. Jairam, N. Cyrus, C. E. Brokowski, S. C. Eisenbarth, G. M. Phillips, G. W. Cline, A. J. Phillips and R. Medzhitov, *Nature*, 2014, **513**, 559–563.
- 80 T. Bohn, S. Rapp, N. Luther, M. Klein, T.-J. Bruehl, N. Kojima, P. A. Lopez, J. Hahlbrock, S. Muth, S. Endo, S. Pektor, A. Brand, K. Renner, V. Popp, K. Gerlach, D. Vogel, C. Lueckel, D. Arnold-Schild, J. Pouyssegur, M. Kreutz, M. Huber, J. Koenig, B. Weigmann, H.-C. Probst, E. von Stebut, C. Becker, H. Schild, E. Schmitt and T. Bopp, *Nat. Immunol.*, 2018, **19**, 1319–1329.
- 81 M. Obeid, A. Tesniere, F. Ghiringhelli, G. M. Fimia, L. Apetoh, J.-L. Perfettini, M. Castedo, G. Mignot, T. Panaretakis, N. Casares, D. Metivier, N. Larochette, P. van Endert, F. Ciccosanti, M. Piacentini, L. Zitvogel and G. Kroemer, *Nat. Med.*, 2007, **13**, 54–61.
- 82 D. V. Krysko, A. D. Garg, A. Kaczmarek, O. Krysko, P. Agostinis and P. Vandenabeele, *Nat. Rev. Cancer*, 2012, **12**, 860–875.
- 83 J. Lu, X. Liu, Y.-P. Liao, X. Wang, A. Ahmed, W. Jiang, Y. Ji, H. Meng and A. E. Nel, *ACS Nano*, 2018, **12**, 11041–11061.
- 84 F. Zhou, B. Feng, H. Yu, D. Wang, T. Wang, Y. Ma, S. Wang and Y. Li, *Adv. Mater.*, 2019, **31**, 1805888.
- 85 X. Duan, C. Chan and W. Lin, *Angew. Chem., Int. Ed.*, 2019, **58**, 670–680.
- 86 P. Zheng, B. Ding, Z. Jiang, W. Xu, G. Li, J. Ding and X. Chen, *Nano Lett.*, 2021, **21**, 2088–2093.
- 87 M. Chang, Z. Hou, M. Wang, C. Li and J. Lin, *Adv. Mater.*, 2020, **33**, 2004788.
- 88 Q. Chen, L. Xu, C. Liang, C. Wang, R. Peng and Z. Liu, *Nat. Commun.*, 2016, **7**, 13193.
- 89 Q. Chen, Q. Hu, E. Dukhovlinova, G. Chen, S. Ahn, C. Wang, E. A. Ogunnaike, F. S. Ligler, G. Dotti and Z. Gu, *Adv. Mater.*, 2019, **31**, 1900192.
- 90 C. W. Ng, J. Li and K. Pu, *Adv. Funct. Mater.*, 2018, **28**, 1804688.
- 91 Z. Liu, S. Zhang, H. Lin, M. Zhao, H. Yao, L. Zhang, W. Peng and Y. Chen, *Biomaterials*, 2018, **155**, 54–63.
- 92 L. Zhou, B. Hou, D. Wang, F. Sun, R. Song, Q. Shao, H. Wang, H. Yu and Y. Li, *Nano Lett.*, 2020, **20**, 4393–4402.
- 93 J. Zhao, S. Ma, Y. Xu, X. Si, H. Yao, Z. Huang, Y. Zhang, H. Yu, Z. Tang, W. Song and X. Chen, *Biomaterials*, 2021, **268**, 120542.

- 94 D. Shae, K. W. Becker, P. Christov, D. S. Yun, A. K. R. Lytton-Jean, S. Sevimli, M. Ascano, M. Kelley, D. B. Johnson, J. M. Balko and J. T. Wilson, *Nat. Nanotechnol.*, 2019, **14**, 269–278.
- 95 A. F. U. H. Saeed, X. Ruan, H. Guan, J. Su and S. Ouyang, *Adv. Sci.*, 2020, **7**, 1902599.
- 96 M. Lv, M. Chen, R. Zhang, W. Zhang, C. Wang, Y. Zhang, X. Wei, Y. Guan, J. Liu, K. Feng, M. Jing, X. Wang, Y.-C. Liu, Q. Mei, W. Han and Z. Jiang, *Cell Res.*, 2020, **30**, 966–979.
- 97 C. Wang, Y. Guan, M. Lv, R. Zhang, Z. Guo, X. Wei, X. Du, J. Yang, T. Li, Y. Wan, X. Su, X. Huang and Z. Jiang, *Immunity*, 2018, **48**, 675–687.
- 98 L. Hou, C. Tian, Y. Yan, L. Zhang, H. Zhang and Z. Zhang, *ACS Nano*, 2020, **14**, 3927–3940.
- 99 B. Ding, S. Shao, C. Yu, B. Teng, M. Wang, Z. Cheng, K.-L. Wong, P. A. Ma and J. Lin, *Adv. Mater.*, 2018, **30**, 1802479.
- 100 R. Kuai, L. J. Ochyl, K. S. Bahjat, A. Schwendeman and J. J. Moon, *Nat. Mater.*, 2017, **16**, 489–496.
- 101 S.-Y. Liu, W. Wei, H. Yue, D.-Z. Ni, Z.-G. Yue, S. Wang, Q. Fu, Y.-Q. Wang, G.-H. Ma and Z.-G. Su, *Biomaterials*, 2013, **34**, 8291–8300.
- 102 S. C. Eisenbarth, O. R. Colegio, W. O'Connor, Jr., F. S. Sutterwala and R. A. Flavell, *Nature*, 2008, **453**, 1122–1126.
- 103 T. L. Flach, G. Ng, A. Hari, M. D. Desrosiers, P. Zhang, S. M. Ward, M. E. Seamone, A. Vilaysane, A. D. Mucsi, Y. Fong, E. Prenner, C. C. Ling, J. Tschopp, D. A. Muruve, M. W. Amrein and Y. Shi, *Nat. Med.*, 2011, **17**, 479–487.
- 104 Y. Wang, Y. Xie, J. Luo, M. Guo, X. Hu, X. Chen, Z. Chen, X. Lu, L. Mao, K. Zhang, L. Wei, Y. Ma, R. Wang, J. Zhou, C. He, Y. Zhang, Y. Zhang, S. Chen, L. Shen, Y. Chen, N. Qiu, Y. Liu, Y. Cui, G. Liao, Y. Liu and C. Chen, *Nano Today*, 2021, **38**, 101139.